

1 **SARS-CoV-2 Triggers Complement Activation through Interactions**
2 **with Heparan Sulfate**

3
4 **Authors:** Martin W. Lo^{1,*}, Alberto A. Amarilla^{2,*}, John D. Lee¹, Eduardo A. Albornoz¹,
5 Naphak Modhiran², Richard J. Clark¹, Vito Ferro^{2,3}, Mohit Chhabra², Alexander A.
6 Khromykh^{2,3}, Daniel Watterson^{2,3}, Trent M. Woodruff¹

7
8 **Affiliations**

9 ¹School of Biomedical Sciences, Faculty of Medicine, University of Queensland, St
10 Lucia, Brisbane, Australia, 4072

11 ²School of Chemistry and Molecular Biosciences, University of Queensland, St Lucia,
12 Brisbane, Australia, 4072

13 ³Australian Infectious Diseases Research Centre, Global Virus Network Centre of
14 Excellence, Brisbane, Australia

15 *equal contribution

16
17 **Correspondence**

18 Professor Trent M. Woodruff (Email: t.woodruff@uq.edu.au)

19 Associate Professor Daniel Watterson (Email: d.watterson@uq.edu.au)

20

21

22

23

24

25

26 **ABSTRACT**

27 The complement system has been heavily implicated in severe COVID-19 with clinical
28 studies revealing widespread gene induction, deposition, and activation. However, the
29 mechanism by which complement is activated in this disease remains incompletely
30 understood. Herein we examined the relationship between SARS-CoV-2 and
31 complement by inoculating the virus in lepirudin-anticoagulated human blood. This
32 caused progressive C5a production after 30 minutes and 24 hours, which was blocked
33 entirely by inhibitors for factor B, C3, C5, and heparan sulfate. However, this
34 phenomenon could not be replicated in cell-free plasma, highlighting the requirement
35 for cell surface deposition of complement and interactions with heparan sulfate.
36 Additional functional analysis revealed that complement-dependent granulocyte and
37 monocyte activation was delayed. Indeed, C5aR1 internalisation and CD11b
38 upregulation on these cells only occurred after 24 hours. Thus, SARS-CoV-2 is a non-
39 canonical complement activator that triggers the alternative pathway through
40 interactions with heparan sulfate.

41

42

43

44

45

46

47

48

49

50

51

52 INTRODUCTION

53 COVID-19 is a highly contagious respiratory infection caused by the severe acute
54 respiratory syndrome coronavirus 2 (SARS-CoV-2). In the last two years, this disease
55 has affected over 300 million individuals and caused over 5.4 million deaths (1). Thus,
56 unprecedented efforts have been put towards vaccine and drug development, but with
57 the possibility of new variants and the inevitability of future pandemics, a fundamental
58 understanding of severe COVID-19 is still needed. In this context, SARS-CoV-2
59 replicates in an unchecked manner and evades the immune system by exploiting
60 several inborn and acquired weaknesses (2, 3). At a critical mass, these virions then
61 trigger a hyperinflammatory response that results in acute respiratory distress
62 syndrome (ARDS) (4). Emerging evidence suggests that the complement system
63 plays a key role in this process (5-7). Indeed, complement activation has been
64 correlated with disease severity (8) and small case studies have shown that
65 complement inhibition can be effective in critical patients, prompting at least six anti-
66 complement drugs to be taken to clinical trials (5). However, whilst *in vitro* mechanistic
67 studies have demonstrated that specific viral proteins can activate complement, the
68 relationship between SARS-CoV-2 and complement activation remains incompletely
69 understood.

70

71 Complement-mediated disease in COVID-19 appears to be confined to severely ill
72 patients who are unable to bring the virus under immunological control. In these
73 patients, SARS-CoV-2 exploits defects in the type 1 interferon system and replicates
74 in an unchecked manner, which at a critical mass, is believed to drive a form of
75 complement-mediated hyperinflammation (3). Indeed, evidence of complement
76 activation has been correlated with disease severity and includes serum C5a and C5b-
77 9 concentrations (8), monocyte and granulocyte CD11b expression (9) which can be

78 due to C5aR1 activation (10, 11), and post-mortem immunochemistry (7, 12). These
79 features occur on the background of airway and intravascular complement synthesis
80 (13, 14) and are particularly prominent in individuals who are genetically prone to C5
81 cleavage (15), who have elevated mannose binding protein levels (16), or who have
82 reduced CD55 expression (17). Additional investigations suggest that complement
83 activation in severe COVID-19 can occur through the classical, lectin, and alternative
84 pathways (18-20). Thus, complement is likely to be a key driver of severe COVID-19.

85

86 Moreover, molecular investigations have provided some insight into the underlying
87 mechanisms that drive complement activation in COVID-19. Indeed, an initial study
88 utilising the SARS-CoV-2 S-protein in a specialised functional assay suggests that the
89 virus may activate the alternative pathway by binding to cell surface heparan sulfate,
90 which disinhibits factor H-mediated complement suppression (21). In this study,
91 normal human serum pre-treated with recombinant SARS-CoV-2 S protein caused
92 complement deposition and cytotoxicity in complement-inhibitor deficient cells.
93 However, SARS-CoV-2 S-protein did not generate complement activation products in
94 human serum without such cells or after heparan sulfate or factor H supplementation.
95 In addition, a more recent study found that the SARS-CoV-2 S and N proteins are able
96 to activate the lectin pathway via MASP-2 (22). Thus, early molecular studies using
97 viral proteins suggest that SARS-CoV-2 can directly activate the complement system,
98 but conclusive evidence for this with live virus is still outstanding.

99

100 Therefore, here we inoculated SARS-CoV-2 into lepirudin-anticoagulated human
101 blood and used ELISAs and flow cytometry to measure complement activation and
102 functionality respectively. We show that SARS-CoV-2 activates complement via the

103 alternative pathway by interacting with heparan sulfate, and in doing so causes
104 delayed leukocyte activation through C5a-C5aR1 signalling.

105

106

107

108

109

110

111

112

113

114

115

116

117

118

119

120

121

122

123

124

125

126

127

128

129 **METHODS**

130 *Study approval*

131 This research was approved by the University of Queensland Human Research Ethics
132 Committee and the University of Queensland Biosafety Committee (supplementary
133 methods 1). All participants gave informed written consent.

134

135 *Participants*

136 Whole blood was drawn from healthy individuals (supplementary table 1) with a 4.9ml
137 S-Monovette (SARSTEDT, Nümbrecht, Germany, # 04.1926.001) and anticoagulated
138 with 50µg/ml Lepirudin (Pharmion, Boulder, California), which is an anticoagulant that
139 permits *ex vivo* complement activation (11). Türk's solution (Sigma-Aldrich, Saint
140 Louis, Missouri, # 109277) was used as per manufacturer guidelines to perform total
141 leukocyte counts for MOI calculations.

142

143 *Whole blood inoculation*

144 For the ELISA experiments, 100µl of whole blood was inoculated with SARS-CoV-2
145 at a MOI of 0.1 or 1.0 (supplementary methods 2), LPS O111:B4 (200µg/ml; Sigma-
146 Aldrich, #L2630-100MG), or a mock solution (i.e., DMEM with 2% HIFCS and P/S) for
147 30 minutes or 24 hours at 37°C. Samples were then centrifuged at 2000g for 10
148 minutes at 4°C and plasma was aliquoted and stored at -80°C for downstream analysis.
149 Certain samples were pre-treated with the following for 30 minutes at 37°C: SFMI-1
150 (MASP1/2 inhibitor 10µM; synthesized in house (23)), LNP023 (factor B inhibitor,
151 10µM; AdooQ Bioscience, Irvine, California, #A18905) compstatin analogue (C3
152 inhibitor, 20µM; Wuxi AppTec Ltd, Shanghai, China, #C15031904), eculizumab (C5
153 inhibitor, 100µg/mL; Ichorbio, Wantage, United Kingdom, #ICH4005), EGCG

154 (heparan sulfate inhibitor, 100 μ M; Sigma-Aldrich E4143-50MG), or pixatimod/PG545
155 (heparan sulfate mimetic, 100 μ g/mL; synthesized in house (24)). This assay was
156 repeated with plasma isolated from whole blood after centrifugation at 2000g for 10
157 minutes at room temperature. For the flow cytometry experiments, whole blood was
158 mixed 1:1 with RPMI1640 (Gibco, Waltham, Massachusetts, #42401-018) and
159 inoculated with SARS-CoV-2 at a MOI of 0.1 or 1.0 or a mock solution (as above) and
160 incubated for 3 or 24 hours at 37°C with 5% CO₂. Certain samples were pre-treated
161 with PMX205 (10 μ M; synthesized as previously described (25)) or eculizumab (as
162 above) for 30 minutes at 37°C with 5% CO₂.

163

164 *ELISA*

165 A C5a ELISA (R&D, Minneapolis, Minnesota, #DY2037) was performed as per
166 manufacturer's guidelines on plasma samples from whole blood inoculated with
167 SARS-CoV-2 for 30 minutes and 24 hours.

168

169 *Flow cytometry*

170 Whole blood inoculated with SARS-CoV-2 was blocked with 5 μ l of TruStain (Biolegend,
171 San Diego, California, # 422302) for 10 minutes at room temperature and then stained
172 for granulocyte and monocyte markers, complement receptors, and viability for 15
173 minutes at room temperature (supplementary methods 3). Samples were then fixed
174 and lysed with 2ml of BD FACSLyse (BD, Franklin Lakes, New Jersey, # 349202) for
175 15 minutes at room temperature and inverted 10 times at the 0- and 7.5-minute marks.
176 Lysed samples were then centrifuged at 600g for 5 minutes at room temperature.
177 Leukocytes were then resuspended in PBS for flow cytometry acquisition on a BD LSR
178 Fortessa II. Data analysis was performed with FlowJo v10.6.2.

179

180 *Statistical analysis*

181 Statistical analysis was performed with GraphPad Prism Software v9.3.1. A one-way
182 ANOVA with Dunnett's post-test analysis was used for one factor ordinal and
183 categorical data. Otherwise, t-tests were used to compare means to assess for
184 temporal differences in functional assays and for drug effects in the context of SARS-
185 CoV-2 inoculation. Additional detail is provided in supplementary methods 4 and the
186 source data file.

187

188

189

190

191

192

193

194

195

196

197

198

199

200

201

202

203

204

205

206 RESULTS AND DISCUSSION

207 *SARS-CoV-2 activates the alternative pathway through interactions with heparan* 208 *sulfate*

209 We first investigated whether SARS-CoV-2 could mediate complement activation by
210 inoculating the virus at multiplicity of infection (MOI) 0.1 and 1.0 in lepirudin-
211 anticoagulated human blood from individuals with no history of COVID-19 or
212 respective vaccination and subsequently measuring plasma C5a with an ELISA.
213 Indeed, inoculated whole blood showed an increase in C5a of 5-10ng/mL and 30-
214 50ng/mL at MOI 1.0 when compared to the mock control at 30 minutes and 24 hours
215 post-inoculation respectively (figure 1a). However, this phenomenon could not be
216 replicated in isolated plasma (figure 1b), which suggests that a cellular component is
217 required. To further delineate the pathways involved, SARS-CoV-2 inoculated whole
218 blood was pre-treated with inhibitors/mimetics, in which antagonism of factor B, C3,
219 C5, and heparan sulfate, and to a lesser extent MASP1/2, attenuated complement
220 activation (figure 2).

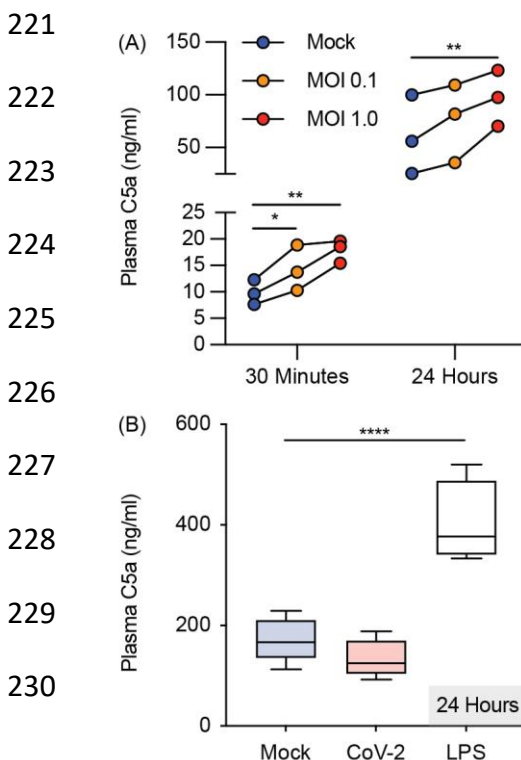


Figure 1. SARS-CoV-2 activates complement in whole blood but not in plasma. Plasma C5a levels were assessed with an ELISA in SARS-CoV-2 inoculated lepirudin-anticoagulated (A) human blood (n = 3) and (B) plasma at indicated times (n = 5). Boxes depict medians and inter-quartile ranges and have Tukey whiskers. MOI = Multiplicity of infection; CoV-2 = SARS-CoV-2 MOI 1.0; * P < 0.05, ** P < 0.01, **** P < 0.0001, using a one-way ANOVA and Dunnett's post-test.

231 Moreover, serological testing confirmed that all blood donors were seronegative for
 232 SARS-CoV-2 and thus excluded any antibody-mediated complement activation via the
 233 classical pathway (figure 2 – figure supplement 1). Thus, given that the C3, C5, and
 234 heparan sulfate inhibitors were membrane impermeable, these findings indicate that
 235 SARS-CoV-2 activates the alternative pathway through interactions with cell surface
 236 heparan sulfate and subsequent plasma complement deposition.

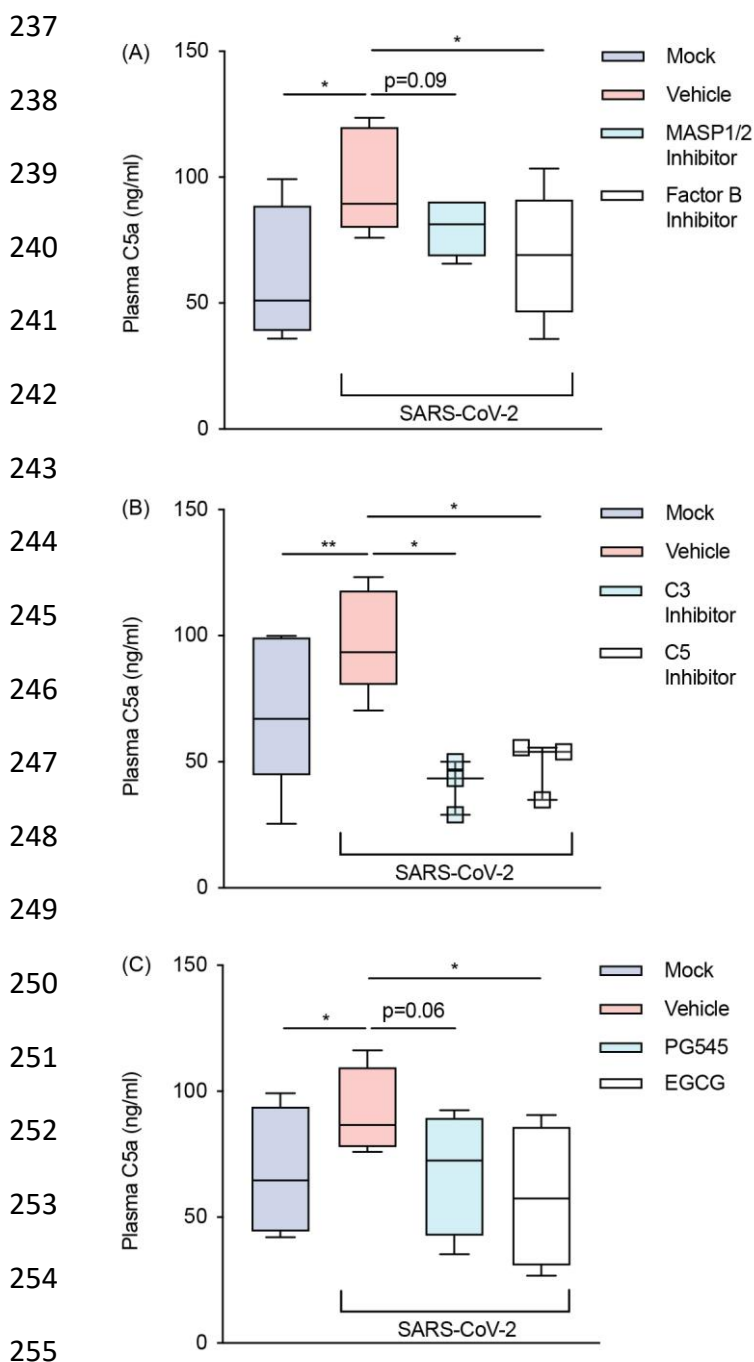


Figure 2. SARS-CoV-2 activates the alternative pathway through interactions with heparan sulfate. Plasma C5a levels were assessed with an ELISA in SARS-CoV-2 inoculated lepirudin-anticoagulated human blood pre-treated with various inhibitors and mimetics. These included antagonists for (A) MASP1/2 (SFMI-1 10 μ M) and factor B (LNP023 10 μ M) (n = 5); (B) C3 (Compstatin 20 μ M) and C5 (Eculizumab 100 μ g/mL) (n = 3); and (C) heparan sulfate (EGCG 100 μ M) as well as a mimetic for heparan sulfate (PG545 100 μ g/mL) (n = 4). SARS-CoV-2 was inoculated at MOI 1.0 for 24 hours. Boxes depict medians and inter-quartile ranges and have Tukey whiskers. Where this was not possible, individual values are presented instead. MOI = multiplicity of infection; * P<0.05, ** P<0.01, using a paired one-tailed t test. All blood donors were seronegative for anti-SARS-CoV-2 antibodies (Figure 2 - figure supplement 1).

256

257 *Flow cytometry optimization and incidental findings on monocyte activation*

258 Next, we sought to determine if SARS-CoV-2-mediated complement activation was
259 sufficient to induce a functional response. As C5a stimulation of myeloid cells causes
260 C5aR1 internalisation and CD11b upregulation at the cell surface (10, 11), we
261 inoculated whole blood with SARS-CoV-2 (MOI 0.1 and 1.0) for 3 and 24 hours and
262 used flow cytometry to measure C5aR1 and CD11b surface expression on neutrophils,
263 eosinophils, and monocytes. To do so, we trialled an optimized flow cytometry panel
264 under inoculation conditions and found gating properties to be slightly altered (figure
265 3 – figure supplement 1) compared to blood inoculated with a mock control. Indeed,
266 whilst granulocyte markers were unaffected, monocyte markers including CD16 and
267 HLA-DR were upregulated in an MOI-dependent fashion (supplementary figure 2a),
268 which suggests that other immune phenomena were present in this assay. Thus, pan-
269 monocytes without subset differentiation were examined in this study.

270

271 *SARS-CoV-2 causes delayed complement-mediated leukocyte activation*

272 Given that immune stimulators induce rapid changes in myeloid cell activation, we first
273 tested whether SARS-CoV-2 could cause complement-mediated leukocyte activation
274 at 3 hours post-inoculation in whole blood. However, at this time point, flow cytometry
275 revealed few alterations in cell activation markers in neutrophils, eosinophils, and
276 monocytes. We therefore extended the period of SARS-CoV-2 incubation to 24 hours
277 and detected significant C5aR1 internalisation and CD11b upregulation on innate
278 leukocytes. This was observed in neutrophils, eosinophils, and monocytes and was
279 most prominent at MOI 1.0 (figure 3). Interestingly, at 3 hours post-inoculation, CD11b
280 upregulation without concomitant C5aR1 internalisation was noted in neutrophils,
281 which suggests that these cells can react acutely to SARS-CoV-2 through receptors
282 independent of complement (figure 3 – figure supplement 2).

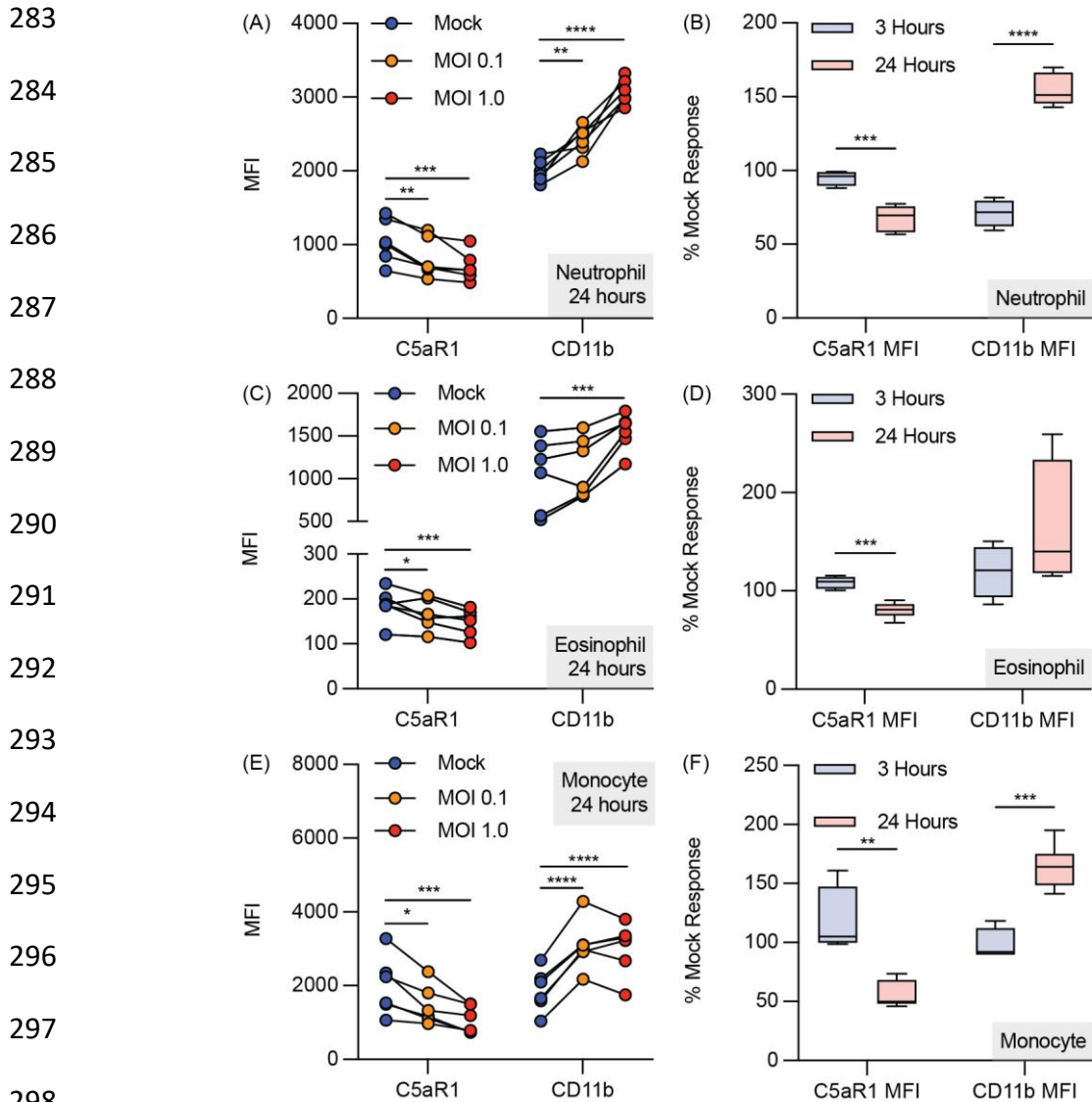


Figure 3. SARS-CoV-2 causes delayed complement-mediated activation in innate leukocytes. SARS-CoV-2 inoculated lepirudin-anticoagulated human blood was analysed with flow cytometry. SARS-CoV-2 caused dose-dependent C5aR1 internalisation and CD11b upregulation in (A) neutrophils, (C) eosinophils, and (E) monocytes at 24 hours post inoculation (n = 6). Comparison of C5aR1 and CD11b responses between SARS-CoV-2 inoculated blood at 3 (n = 4) and 24h (n = 6) expressed as a percentage change from mock inoculation (B, D, F). Boxes depict medians and inter-quartile ranges and have Tukey whiskers. MOI = multiplicity of infection; * P<0.05, ** P<0.01, *** P<0.001, **** P<0.0001 using a one-way ANOVA and Dunnett's post-test or unpaired t test with two stage step-up 1% false discovery rate correction. Flow cytometry gating strategy and incidental findings are provided (Figure 3 – figure supplement 1 and 2).

305
306
307
308

309 *Anti-C5/C5aR1 drugs eculizumab and PMX205 inhibit SARS-CoV-2-induced*
310 *complement-mediated inflammation*

311 To investigate the functional role of the terminal complement pathway in mediating
312 leukocyte activation in response to SARS-CoV-2, we next pre-incubated whole blood
313 with a C5 inhibitor (eculizumab) and a C5aR1 antagonist (PMX205). At 24 hours post
314 inoculation, both drugs inhibited SARS-CoV-2-dependent C5aR1 internalisation and
315 CD11b upregulation in neutrophils and eosinophils with similar efficacy (figure 4a-b).
316 By contrast, on monocytes, these drugs were only able to partially inhibit C5aR1
317 internalisation and did not lower CD11b upregulation (figure 4b). This latter finding
318 suggests that complement at the level of C5 is not involved in this process in
319 monocytes.

320

321

322

323

324

325

326

327

328

329

330

331

332

333

334

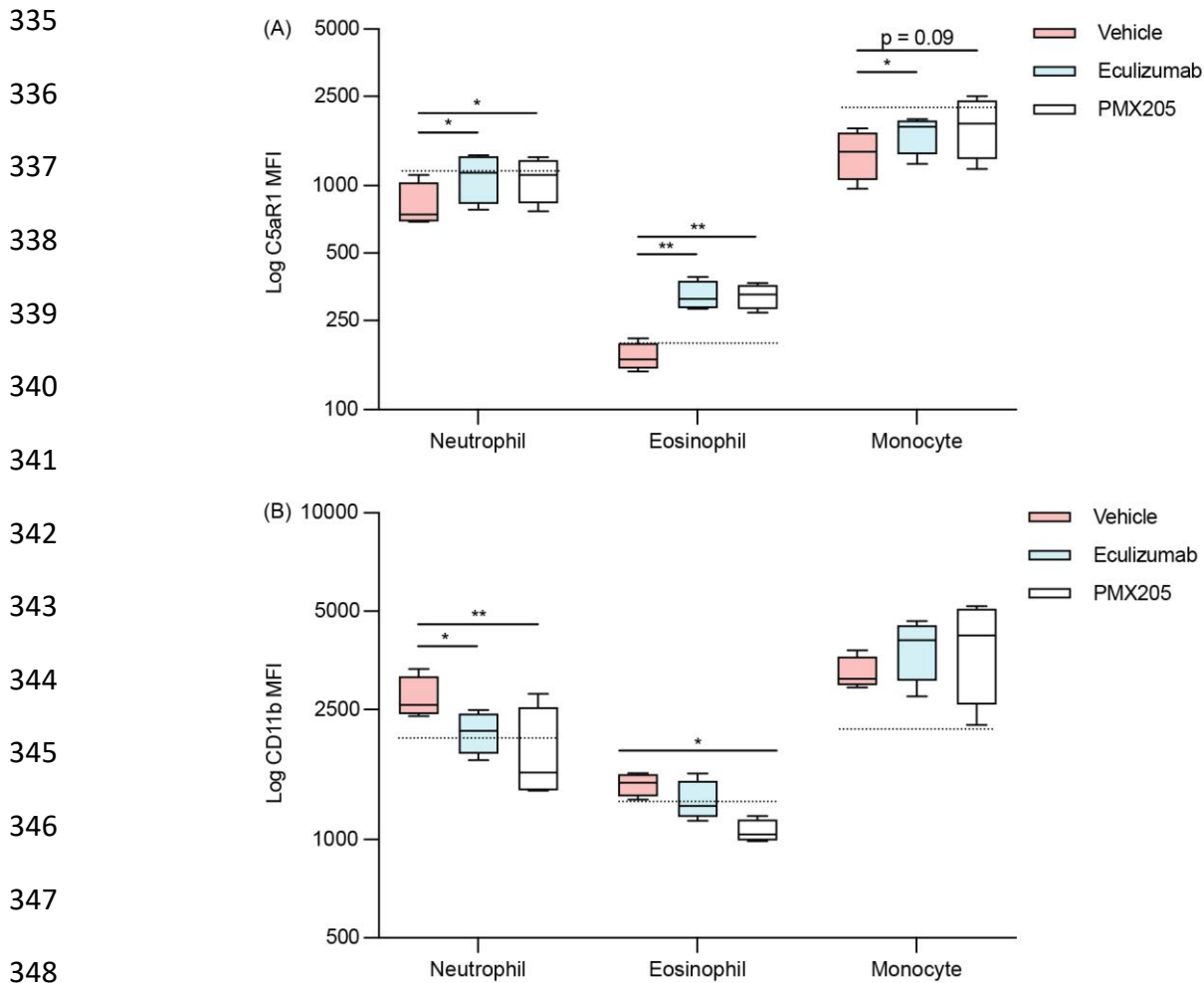


Figure 4. C5/C5aR1 inhibition attenuates SARS-CoV-2-induced leukocyte activation. Anti-C5/C5aR1 inhibitors eculizumab (100 μ g/mL) and PMX205 (10 μ M) were administered to lepirudin-anticoagulated whole blood (n = 4) prior to SARS-CoV-2 inoculation at MOI 1.0 for 24 hours and analysed with flow cytometry. Activation markers C5aR1 and CD11b were measured as MFI. Boxes depict medians and inter-quartile ranges and have Tukey whiskers. The dashed line represents the mock infection baseline. MOI = multiplicity of infection; MFI = median fluorescence intensity; * P < 0.05, ** P < 0.01, using a paired one-tailed t test.

Results support clinical findings of complement in COVID-19

Overall, the complement activation observed in our *ex-vivo* blood study is consistent with the current clinical and molecular understanding of COVID-19. Foremost, *in vivo* complement profiling in severe COVID-19 reveals hyperactivation of the alternative pathway (14, 19) and *in vitro* studies have shown that viral S-protein can activate this same pathway through interactions with heparan sulfate (21). However, in contrast to our *ex vivo* model, complement activation during COVID-19 is probably a multifactorial phenomenon driven by multiple complement pathways (7, 20, 22), non-specific DAMP

361 release (5), genetic susceptibility to complement activation (15-17), and local
362 complement synthesis (13). But in this regard, our participants were seronegative for
363 anti-SARS-CoV-2 antibodies, which would imply that the classical pathway was not
364 activated in this study. Additionally, given that C5a-mediated immune activation
365 typically occurs within 60 minutes (11, 26), the delayed response requiring 24 hours
366 in our model is consistent with the gradual progression (4) and upregulation of CD11b
367 on leukocytes in severe cases (9). Thus, these results strongly support the emerging
368 paradigm of heparan sulfate- and alternative pathway-mediated disease in severe
369 COVID-19.

370

371 *Complement activation appears to be localised to organs that support replication*

372 When placed in the context of *in vivo* viral titres, our results also suggest that SARS-
373 CoV-2-mediated complement activation is localized to organs that can support
374 replication. On average COVID-19 patients have median viral titres of $\sim 10^6$ RNA
375 copies/ml in their airways; as determined from nasopharyngeal swaps, sputum, saliva,
376 and bronchoalveolar lavage fluid; and $\sim 10^3$ RNA copies/ml in their serum, in which the
377 former is at least 10 times higher in severe cases compared to that in mild cases (27,
378 28). By comparison, in this study whole blood inoculated with SARS-CoV-2 at MOI 0.1
379 and 1.0 was exposed to virion concentrations of $\sim 3.5-5.5 \times 10^5$ and $\sim 3.5-5.5 \times 10^6$
380 FFU/ml respectively. Thus, complement activation in severe COVID-19 is most likely
381 localised to tissues that support replication (e.g., lung parenchyma) with changes in
382 plasma complement occurring as a secondary phenomenon. This implies that anti-
383 complement drugs in severe COVID-19 require significant tissue
384 distribution/permeation, which may have been a limiting factor for the parenteral drugs
385 that have so far been tested in clinical trials. In this sense, SARS-CoV-2 can be viewed

386 as an organ-based activator of complement that poses unique challenges to drug
387 development.

388

389 *Complement and heparan sulfate in severe COVID-19*

390 Furthermore, complement activation through heparan sulfate appears to be an
391 inadvertent phenomenon. Indeed, this polysaccharide post-translational modification
392 promotes specific protein-protein interactions, which in this case concentrates factor
393 H on host cells to prevent excessive complement activation (29). Therefore, whilst
394 SARS-CoV-2 principally uses heparan sulfate to dock with angiotensin-converting
395 enzyme 2 to enable infection (30), it also secondarily activates complement by causing
396 factor H disinhibition. In our *ex vivo* model, this was largely mediated by CD44v3 on
397 lymphocytes, but *in vivo* is probably the result of interactions with a range of membrane
398 bound (e.g., syndecan 1-4 and glypican 1-6) and extracellular matrix proteoglycans
399 (e.g., perlecan, agrin, and collagen XVII) (31). Interestingly, S protein can bind to
400 heparan sulfate and disrupt anti-thrombin and heparin cofactor II activity and thus this
401 polysaccharide modification warrants further investigation as a multi-faceted drug
402 target in severe COVID-19 (32).

403

404 *Concluding remarks*

405 COVID-19 continues to cause more deaths than any other pandemic in living memory.
406 Mounting evidence suggests that complement plays a key role in its most severe form
407 and here we show that SARS-CoV-2 interacts with heparan sulfate to activate the
408 alternative pathway, which ultimately drives innate leukocyte activation through C5a-
409 C5aR1 signalling. In doing so, these findings support the use of targeted anti-
410 complement treatments in severe COVID-19.

411

412 **AUTHORSHIP CONTRIBUTIONS**

413 MWL* designed the project, recruited healthy participants, managed logistics, ran the
414 flow cytometry samples, analysed the data, made the figures, and drafted the
415 manuscript.

416 AAA* contributed to experimental design, conducted all experimental work within the
417 biosafety level 3 facility, and drafted the methods section for this.

418 JDL contributed ideas, validated reagents, and edited the final manuscript.

419 EAA edited the final manuscript and assisted AAA in experimental planning.

420 NM performed serology experiments and drafted the methods section for this.

421 RJC synthesized SFMI-1.

422 MC synthesized Pixatimod/PG545 under the supervision of VF.

423 AAK oversaw SARS-CoV-2 laboratory setup and assay development, provided
424 funding and edited the final manuscript.

425 DW oversaw the SARS-CoV-2 experimental studies, provided funding, and edited the
426 final manuscript.

427 TMW co-conceived the idea for the project, contributed to experimental design,
428 oversaw the entire study, provided funding, helped design figures, and contributed
429 substantial edits to the drafted manuscript.

430 The order of co-first authorship* was based on the intellectual contribution to the
431 manuscript.

432

433

434

435

436

437

438 **ACKNOWLEDGMENTS**

439 We would like to thank the Queensland Health Forensic and Scientific Services,
440 Queensland Department of Health, for providing the QLD02 SARS-CoV-2 isolate. We
441 acknowledge funding support from the National Health and Medical Research Council
442 (APP1118881), The Australian Infectious Diseases Research Centre (COVID-19 seed
443 grant to AAK), and the Medical Research Future Fund (APP1202445-2020 MRFF
444 Novel Coronavirus Vaccine Development Grant).

445

446 **COMPETING INTERESTS**

447 Trent M. Woodruff is an inventor on patents pertaining to complement inhibitors for
448 inflammatory diseases. He has consulted to Alsonex Pty Ltd (who are commercially
449 developing PMX205) and has received honorarium from Alexion Pharmaceuticals
450 (who developed eculizumab) for participation in industry conferences and meetings.
451 Vito Ferro is an inventor on patents for Pixatimod/PG545. All other authors declare no
452 conflicts of interest.

453

454

455

456

457

458

459

460

461

462

463

464 REFERENCES

- 465 1. Dong E, Du H, Gardner L. An interactive web-based dashboard to track
466 COVID-19 in real time. *The Lancet Infectious Diseases*. 2020;20(5):533-4.
- 467 2. Taefehshokr N, Taefehshokr S, Hemmat N, Heit B. Covid-19: Perspectives on
468 Innate Immune Evasion. *Frontiers in immunology*. 2020;11(2549).
- 469 3. Hadjadj J, Yatim N, Barnabei L, Corneau A, Boussier J, Smith N, et al.
470 Impaired type I interferon activity and inflammatory responses in severe COVID-19
471 patients. *Science (New York, NY)*. 2020;369(6504):718-24.
- 472 4. Berlin DA, Gulick RM, Martinez FJ. Severe Covid-19. *New England Journal of*
473 *Medicine*. 2020.
- 474 5. Lo MW, Kemper C, Woodruff TM. COVID-19: Complement, Coagulation, and
475 Collateral Damage. *The Journal of Immunology*. 2020;ji2000644.
- 476 6. Woodruff TM, Shukla AK. The Complement C5a-C5aR1 GPCR Axis in
477 COVID-19 Therapeutics. *Trends in immunology*. 2020;41(11):965-7.
- 478 7. Satyam A, Tsokos MG, Brook OR, Hecht JL, Moulton VR, Tsokos GC.
479 Activation of classical and alternative complement pathways in the pathogenesis of
480 lung injury in COVID-19. *Clinical Immunology*. 2021:108716.
- 481 8. Ma L, Sahu SK, Cano M, Kuppuswamy V, Bajwa J, McPhatter JN, et al.
482 Increased complement activation is a distinctive feature of severe SARS-CoV-2
483 infection. *Science Immunology*. 2021;6(59):eabh2259.
- 484 9. Gupta R, Gant VA, Williams B, Enver T. Increased Complement Receptor-3
485 levels in monocytes and granulocytes distinguish COVID-19 patients with pneumonia
486 from those with mild symptoms. *International Journal of Infectious Diseases*. 2020.
- 487 10. Herrmann JB, Muenstermann M, Strobel L, Schubert-Unkmeir A, Woodruff
488 TM, Gray-Owen SD, et al. Complement C5a Receptor 1 Exacerbates the
489 Pathophysiology of *N. meningitidis* Sepsis and Is a Potential Target for Disease
490 Treatment. *mBio*. 2018;9(1):e01755-17.
- 491 11. Mollnes TE, Brekke OL, Fung M, Fure H, Christiansen D, Bergseth G, et al.
492 Essential role of the C5a receptor in *E coli*-induced oxidative burst and phagocytosis
493 revealed by a novel lepirudin-based human whole blood model of inflammation.
494 *Blood*. 2002;100(5):1869-77.
- 495 12. Pfister F, Vonbrunn E, Ries T, Jäck H-M, Überla K, Lochnit G, et al.
496 Complement Activation in Kidneys of Patients With COVID-19. *Frontiers in*
497 *immunology*. 2021;11(3833).
- 498 13. Yan B, Freiwald T, Chauss D, Wang L, West E, Mirabelli C, et al. SARS-CoV-
499 2 drives JAK1/2-dependent local complement hyperactivation. *Science Immunology*.
500 2021;6(58).
- 501 14. Boussier J, Yatim N, Marchal A, Hadjadj J, Charbit B, El Sissy C, et al. Severe
502 COVID-19 is associated with hyperactivation of the alternative complement pathway.
503 *The Journal of allergy and clinical immunology*. 2021.
- 504 15. Valenti L, Griffini S, Lamorte G, Grovetti E, Uceda Renteria SC, Malvestiti F,
505 et al. Chromosome 3 cluster rs11385942 variant links complement activation with
506 severe COVID-19. *Journal of Autoimmunity*. 2021;117:102595.
- 507 16. Eriksson O, Hultström M, Persson B, Lipcsey M, Ekdahl KN, Nilsson B, et al.
508 Mannose-Binding Lectin is Associated with Thrombosis and Coagulopathy in
509 Critically Ill COVID-19 Patients. *Thrombosis and haemostasis*. 2020.
- 510 17. Ramlall V, Thangaraj PM, Meydan C, Foox J, Butler D, Kim J, et al. Immune
511 complement and coagulation dysfunction in adverse outcomes of SARS-CoV-2
512 infection. *Nature medicine*. 2020.

- 513 18. Jarlhelt I, Nielsen SK, Jahn CXH, Hansen CB, Pérez-Alós L, Rosbjerg A, et al.
514 SARS-CoV-2 Antibodies Mediate Complement and Cellular Driven Inflammation.
515 *Frontiers in immunology*. 2021;12(4612).
- 516 19. Charitos P, Heijnen I, Egli A, Bassetti S, Trendelenburg M, Osthoff M.
517 Functional Activity of the Complement System in Hospitalized COVID-19 Patients: A
518 Prospective Cohort Study. *Frontiers in immunology*. 2021;12:765330.
- 519 20. Defendi F, Leroy C, Epaulard O, Clavarino G, Vilotitch A, Le Marechal M, et
520 al. Complement Alternative and Mannose-Binding Lectin Pathway Activation Is
521 Associated With COVID-19 Mortality. *Frontiers in immunology*. 2021;12:742446.
- 522 21. Yu J, Yuan X, Chen H, Chaturvedi S, Braunstein EM, Brodsky RA. Direct
523 activation of the alternative complement pathway by SARS-CoV-2 spike proteins is
524 blocked by factor D inhibition. *Blood*. 2020.
- 525 22. Ali YM, Ferrari M, Lynch NJ, Yaseen S, Dudler T, Gragerov S, et al. Lectin
526 Pathway Mediates Complement Activation by SARS-CoV-2 Proteins. *Frontiers in*
527 *immunology*. 2021;12:714511.
- 528 23. Kocsis A, Kekesi KA, Szasz R, Vegh BM, Balczer J, Dobo J, et al. Selective
529 inhibition of the lectin pathway of complement with phage display selected peptides
530 against mannose-binding lectin-associated serine protease (MASP)-1 and -2:
531 significant contribution of MASP-1 to lectin pathway activation. *Journal of*
532 *immunology (Baltimore, Md : 1950)*. 2010;185(7):4169-78.
- 533 24. Chhabra M, Wimmer N, He QQ, Ferro V. Development of Improved Synthetic
534 Routes to Pixatimod (PG545), a Sulfated Oligosaccharide-Steroid Conjugate.
535 *Bioconjugate Chemistry*. 2021;32(11):2420-31.
- 536 25. Li XX, Lee JD, Massey NL, Guan C, Robertson AAB, Clark RJ, et al.
537 Pharmacological characterisation of small molecule C5aR1 inhibitors in human cells
538 reveals biased activities for signalling and function. *Biochemical pharmacology*.
539 2020;180:114156.
- 540 26. Brekke OL, Christiansen D, Fure H, Fung M, Mollnes TE. The role of
541 complement C3 opsonization, C5a receptor, and CD14 in *E. coli*-induced up-
542 regulation of granulocyte and monocyte CD11b/CD18 (CR3), phagocytosis, and
543 oxidative burst in human whole blood. *Journal of leukocyte biology*. 2007;81(6):1404-
544 13.
- 545 27. Zheng S, Fan J, Yu F, Feng B, Lou B, Zou Q, et al. Viral load dynamics and
546 disease severity in patients infected with SARS-CoV-2 in Zhejiang province, China,
547 January-March 2020: retrospective cohort study. *BMJ*. 2020;369:m1443.
- 548 28. Tsukagoshi H, Shinoda D, Saito M, Okayama K, Sada M, Kimura H, et al.
549 Relationships between Viral Load and the Clinical Course of COVID-19. *Viruses*.
550 2021;13(2).
- 551 29. Loeven MA, Rops AL, Berden JH, Daha MR, Rabelink TJ, van der Vlag J. The
552 role of heparan sulfate as determining pathogenic factor in complement factor H-
553 associated diseases. *Molecular immunology*. 2015;63(2):203-8.
- 554 30. Clausen TM, Sandoval DR, Spliid CB, Pihl J, Perrett HR, Painter CD, et al.
555 SARS-CoV-2 Infection Depends on Cellular Heparan Sulfate and ACE2. *Cell*.
556 2020;183(4):1043-57.e15.
- 557 31. Sarrazin S, Lamanna WC, Esko JD. Heparan sulfate proteoglycans. *Cold*
558 *Spring Harbor Perspectives in Biology*. 2011;3(7).
- 559 32. Zheng Y, Zhao J, Li J, Guo Z, Sheng J, Ye X, et al. SARS-CoV-2 spike
560 protein causes blood coagulation and thrombosis by competitive binding to heparan
561 sulfate. *International Journal of Biological Macromolecules*. 2021;193:1124-9.

- 562 33. Amarilla AA, Modhiran N, Setoh YX, Peng NYG, Sng JDJ, Liang B, et al. An
563 Optimized High-Throughput Immuno-Plaque Assay for SARS-CoV-2. *Frontiers in*
564 *microbiology*. 2021;12(75).
- 565 34. Brekke OL, Hellerud BC, Christiansen D, Fure H, Castellheim A, Nielsen EW,
566 et al. *Neisseria meningitidis* and *Escherichia coli* are protected from leukocyte
567 phagocytosis by binding to erythrocyte complement receptor 1 in human blood.
568 *Molecular immunology*. 2011;48(15-16):2159-69.
- 569 35. Watterson D, Wijesundara DK, Modhiran N, Mordant FL, Li Z, Avumegah MS,
570 et al. Preclinical development of a molecular clamp-stabilised subunit vaccine for
571 severe acute respiratory syndrome coronavirus 2. *Clinical & Translational*
572 *Immunology*. 2021;10(4):e1269.

573
574

575

576

577

578

579

580

581

582

583

584

585

586

587

588

589

590

591

592

593

594 **SUPPLEMENTARY MATERIAL**

C5a ELISA 30min		C5a ELISA 24h		C5a ELISA Pathways	
<i>Sex</i>	<i>Age (Years)</i>	<i>Sex</i>	<i>Age (Years)</i>	<i>Sex</i>	<i>Age (Years)</i>
Male	30	Male	40	Female	20
Male	23	Male	26	Female	20
Female	21	Male	36	Male	31
				Male	27
				Female	57
Flow Cytometry 3h		Flow Cytometry 24h			
<i>Sex</i>	<i>Age (Years)</i>	<i>Sex</i>	<i>Age (Years)</i>		
Male	36	Male	32		
Male	41	Male	24		
Male	25	Male	30		
Female	26	Female	19		
		Male	23		
		Female	25		

595 **Supplementary Table 1: Research Participants for this Study.** Participants were
 596 recruited from the local Brisbane area and had no history of COVID-19, no history
 597 of acute illness or vaccination in the last 2 weeks, no immunodeficiencies or
 598 autoinflammatory/autoimmune conditions, and were not on any immunomodulatory
 599 medications (e.g., corticosteroids). No significant sex or age differences were found
 600 between the cohorts at different time points for the ELISA and flow cytometry
 601 experiments.
 602

603
 604
 605
 606
 607
 608
 609
 610
 611

612
613
614
615
616
617
618
619
620
621
622
623
624
625
626
627
628
629
630
631
632
633
634
635
636
637
638
639
640
641
642
643
644
645
646
647
648
649
650
651
652
653
654
655
656
657
658
659
660
661
662

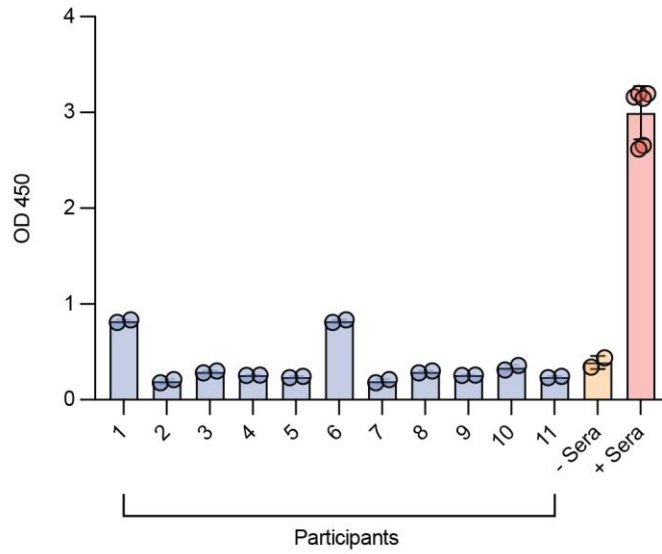


Figure 2 – figure supplement 1. SARS-CoV-2 serology testing of plasma from whole blood used for C5a ELISA studies. Pre-COVID-19 serum (- Sera) was used as a negative control and a biological standard NIBSC 20/130 (+ Sera) was used as a positive control. The data here are from samples diluted at 1:10. Full methods are provided in supplementary methods 5; OD 450 = optical density at the wavelength of 450nm

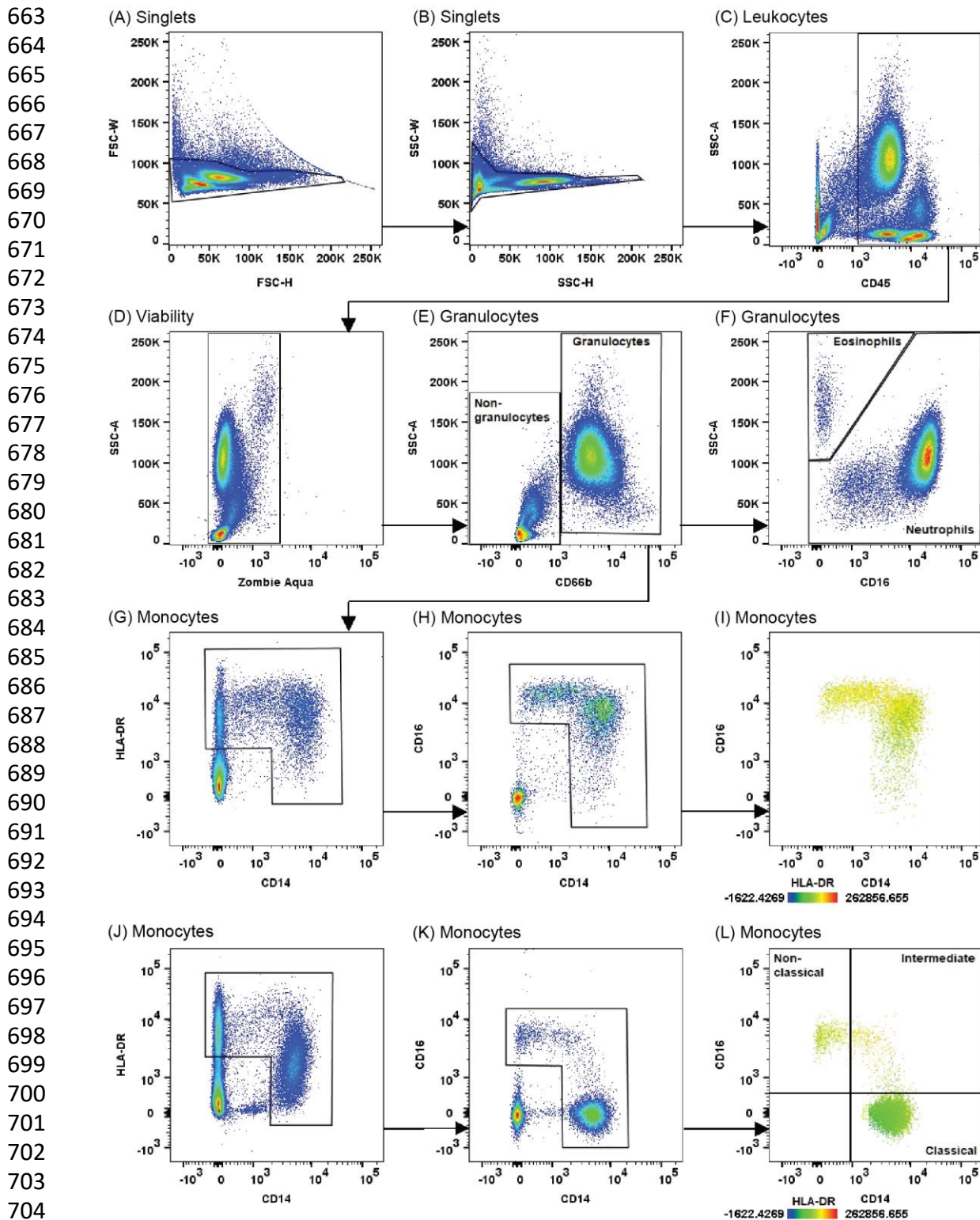


Figure 3 – figure supplement 1. Flow cytometry gating strategy. Representative plots of SARS-CoV-2 inoculated whole blood stained with fluorophore-antibodies and a viability dye for flow cytometry (A-I). For comparison, representative plots of virus-naïve whole blood stained in the same fashion are also provided for the monocyte gates (J-L). All samples had >95% leukocyte viability.

714
715
716
717
718
719
720
721
722
723
724
725
726
727
728
729
730
731
732
733
734
735
736
737
738
739
740
741
742
743
744
745
746
747
748
749
750
751
752
753
754
755
756
757
758
759
760
761
762
763
764

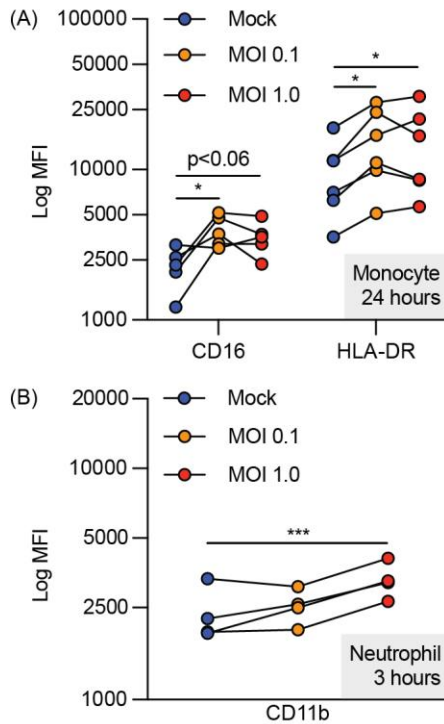


Figure 3 – figure supplement 2.

Upregulation of (A) CD16 and HLA-DR on monocytes and (B) CD11b on neutrophils exposed to SARS-CoV-2. SARS-CoV-2 inoculated lepirudin-anticoagulated whole blood was analysed with flow cytometry at 24 (n = 5-6) and 3 hours post-inoculation (n = 4) respectively. Surface markers were quantified as MFI. MOI = multiplicity of infection; MFI = median fluorescence intensity; * P<0.05, *** P<0.001 using a one-way ANOVA and Dunnett's post-test.

765 **Supplementary Methods 1: Institutional Approval**

766 This research was approved by the University of Queensland Human Research Ethics
767 Committee (TW00105) and the University of Queensland Biosafety Committee
768 (IBC/390B/SCMB/2020, IBC/1301/SCMB/2020, IBC/376B/SBMS/2020 and
769 IBC/447B/SCMB/2021). All experiments were performed in the biosafety level 3 facility
770 at the School of Chemistry and Molecular Biosciences at The University of
771 Queensland, Australia.

772

773 **Supplementary Methods 2: Cell Line and Virus**

774 An African green monkey kidney cell line (Vero E6 cells) was cultured in DMEM (Gibco)
775 supplemented with 10% heat inactivated foetal calf serum (HIFCS) (Bovogen,
776 Melbourne, Australia) and 100U/mL of penicillin and 100µg/mL of streptomycin (P/S).
777 Cells were maintained at 37 °C with 5 % CO₂. The Queensland SARS-CoV-2 isolate
778 QLD02 (GISAID accession EPI_ISL_407896) was recovered from a patient on
779 30/01/2020 by the Queensland Health Forensic & Scientific Services. VeroE6 cells
780 were then inoculated with this isolate and an aliquot (passage 2) was provided. Viral
781 stock (passage 3) was then generated through inoculation of VeroE6 cells in DMEM
782 with 2% HIFCS and P/S and stored at -80 °C. The viral titre was determined by an
783 immuno-plaque assay (iPA) as previously described (33).

784

785

786 **Supplementary Methods 3: Flow Cytometry Staining Reagents**

787 Reagents included CD14-PerCP-Cy5.5 (Biolegend, # 301824), CD16 APC-Cy7
788 (Biolegend, # 302018), HLA-DR BV785 (Biolegend, # 307642), CD88 (C5aR1) PE-
789 Cy7 (Biolegend, # 344308), CD45 BV605 (Biolegend, # 368524), CD66b FITC
790 (Biolegend, # 305104), CD11b AF700 (Biolegend, # 301356), and Zombie Aqua
791 (Biolegend, #423102).

792

793 **Supplementary Methods 4: Statistical Analysis**

794 Initially, a sample size of 3 was determined to be most appropriate for this study. This
795 was decided in reference to previous *ex vivo* complement experiments that have been
796 conducted with the lepirudin whole blood system (34). However, we also generated
797 additional biological replicates according to donor availability and achieved final
798 sample sizes of between 3 and 6.

799

800 Each experiment was performed on one occasion and all data reflects biological
801 replication except for that in supplementary figure 3, in which data points reflect
802 technical replication. Biological and technical replication was defined as the replication
803 of an assay in a blood sample from a distinct or the same donor respectively. One
804 outlier was excluded in supplementary figure 2a as its mock data point was more than
805 3 standard deviations from the mean. No other data was excluded.

806

807 **Supplementary Methods 5: SARS-CoV-2 Serology Testing**

808 Trimeric SARS-CoV-2 spike protein was coated at 2 µg/ml on an ELISA plate overnight
809 (35). Plates were blocked for 1 hour at room temperature with a blocking buffer (PBS
810 containing 0.05% Tween-20 and milk sera diluent/blocking solution (Seracare, Milford,
811 Massachusetts)). Plasma from the whole blood used for the C5a ELISA study, a
812 positive plasma control NIBSC 20/130 and a pre-COVID-19 serum negative
813 control were serially diluted in blocking buffer and added to the plate for 1 hour at 37
814 °C. Plates were washed and probed by goat anti-human HRP antibody (1:2500) in
815 blocking buffer for 1 hour in 37 °C. Tetramethylbenzidine substrate solution and

816 sulfuric acid stop solution were then added prior to absorbance analysis. NIBSC
817 20/130A is a human covalence serum obtained from National Institute for Biological
818 Standards and Control (URL: <https://www.nibsc.org/documents/ifu/20-130.pdf>).